Enhanced Sintering of TiNi Shape Memory Foams under Mg Vapor Atmosphere

TARIK AYDOĞMUŞ and ŞAKIR BOR

TiNi alloy foams are promising candidates for biomaterials to be used as artificial orthopedic implant materials for bone replacement applications in biomedical sector. However, certain problems exist in their processing routes, such as formation of unwanted secondary intermetallic phases leading to brittleness and deterioration of shape memory and superelasticity characteristics; and the contamination during processing resulting in oxides and carbonitrides which affect mechanical properties negatively. Moreover, the eutectic reaction present in Ti-Ni binary system at 1391 K (1118 °C) prevents employment of higher sintering temperatures (and higher mechanical properties) even when equiatomic prealloyed powders are used because of Ni enrichment of TiNi matrix as a result of oxidation. It is essential to prevent oxidation of TiNi powders during processing for high-temperature (>1391 K *i.e.*, 1118 °C) sintering practices. In the current study, magnesium powders were used as space holder material to produce TiNi foams with the porosities in the range of 40 to 65 pct. It has been found that magnesium prevents secondary phase formation and contamination. It also prevents liquid phase formation while enabling employment of higher sintering temperatures by two-step sintering processing: holding the sample at 1373 K (1100 °C) for 30 minutes, and subsequently sintering at temperatures higher than the eutectic temperature, 1391 K (1118 °C). By this procedure, magnesium may allow sintering up to temperatures close to the melting point of TiNi. TiNi foams produced with porosities in the range of 40 to 55 pct were found to be acceptable as implant materials in the light of their favorable mechanical properties.

DOI: 10.1007/s11661-012-1350-y

I. INTRODUCTION

TiNi shape memory foams have a great potential to be used for various applications in biomedical industry, such as artificial hip and orthopedic implant materials for bone replacement applications, because of their shape memory and superelasticity properties as well as their good biocompatibility.[1,2] However, they must also meet the main prospects expected from a biomaterial in terms of strength, ductility, toughness, and Young's modulus. Moreover, they should have interconnected open pores with sizes in the range of 100 to 600 μm[3] and a high porosity to facilitate bone ingrowth after implantation.

Several powder metallurgy techniques have been employed to produce TiNi foams over the last three decades. However, still there exist problems that have to be overcome to fulfill the essential requirements mentioned above for biomedical applications. The prevalent problems are limited pore size and porosity, formation of undesired secondary intermetallic phases leading to brittleness and deterioration of shape memory and superelasticity properties, irregular pore shapes, and inhomogeneous pore distribution resulting in stress concentration and accordingly degradation in mechanical properties, and the contamination during processing resulting in oxides and carbonitrides. For example, conventional sintering (CS) produces TiNi foams with small, irregular pores,[4–8] while self-propagating high-temperature synthesis (SHS) creates anisotropic pore structure.[8,9] Both methods are also unsatisfactory from the point of mechanical properties. Hot isostatic pressing (HIP) suffers from limited porosity and unsuitable pore shapes[10–13] like spark plasma sintering (SPS).[14] Contamination is quite severe because of usage of polymer-based binders in metal injection molding (MIM)[15,16] and also mechanical characteristics are not sufficient for biomedical applications.

Space holder technique (SHT)[17–22] employed with either HIP or CS seems to be best to fabricate TiNi foams with desired pore features and mechanical properties. However, they also result in formation of secondary intermetallic phases like all the alternative processing routes even when prealloyed powders are used.[23–25] Another problem of SHT is formation of two types of pores: micropores resulting from incomplete sintering and macro-pores formed by removal of space holder material.[26] Micropores although favor transportation of body fluids they are not adequate in size to allow bone ingrowth and in fact, they are the origin of inferior mechanical properties. Elimination of micropores completely could be possible by combining SHT

TARIK AYDOĞMUŞ, Research Assistant, is with the Department of Mechanical Engineering, Yüzüncü Yıl University, 65080 Van, Turkey. Contact e-mail: aydogmus@yyu.edu.tr ŞAKIR BOR, Professor, is with the Department of Metallurgical and Materials Engineering, Middle East Technical University, 06531 Ankara, Turkey.

Manuscript submitted December 13, 2011.
Article published online August 7, 2012

with HIP. However, in addition to aforementioned common problems, operational cost of HIP is quite high. As sintering is a diffusion phenomenon, elimination or minimization of micropores can be attained by elevation of the sintering temperature or operating for prolonged sintering time. Former is much more effective because diffusion rate is affected exponentially from temperature. Unfortunately, eutectic reaction present in Ti-Ni binary system at 1391 K (1118 °C) prevents employment of higher sintering temperatures even when equiatomic prealloyed powders are used because of Ni enrichment of TiNi matrix as a result of oxidation as explained by Zhang *et al*.[27] When the eutectic temperature is reached during heating, liquid phase formation occurs resulting in collapse of the compacted powder mixture. Hence TiNi sintering practices are usually carried out at temperatures lower than 1391 K (1118 °C) for both elemental and prealloyed powder sintering.

Bertheville,[6] was the first who produced porous single phase TiNi alloy free from secondary intermetallics using calcium as reductant during sintering in argon atmosphere. He also used the same method to produce bulk TiNi alloys.[28,29] In these studies elemental Ni and Ti/TiH_2 powders have been used as starting powders unlike in the current study. We preferred prealloyed powders produced via inert gas atomization process and magnesium both as reductant and space holder material. Calcium provides a better protective atmosphere since it can decrease the partial pressure of oxygen extremely lower levels. However, its boiling point [1757 K (1484 °C)] is higher than that of magnesium [1363 K (1090 °C)] and thus it may not be removed completely from the structure during sintering.

This paper describes the solutions proposed to the above mentioned general problems in production of TiNi foams by using magnesium powder as space former and explaining the role of magnesium to hinder formation of secondary intermetallics and contamination. In addition, possibility of employment of sintering temperatures higher than the eutectic by usage of magnesium is presented. Finally, improved mechanical properties at higher porosities are introduced.

II. MATERIALS AND METHODS

Starting prealloyed TiNi powders (Ti-50.6 at. pct Ni, 99.9 pct purity, spherical, 1 to 100 μm, supplied by Nanoval GmbH & Co. KG) and magnesium powders (99.82 pct purity, spherical, 250 to 600 μm, supplied by Tangshan Weihao Magnesium Powder Co. Ltd.) as well as the compaction (cold pressing at 400 MPa) and sintering procedures (10 °C/minutes heating rate) except the sintering time and temperature were the same with the ones used in a previous study.[26] In the current study, instead of 1 hour, specimens were sintered for 2 hour at 1473 K (1200 °C) in addition to sintering at 1373 K (1100 °C). Amount of magnesium added in the mixture as space holder was chosen as 30, 40, 50 and 60 pct (by volume) to produce high porosity TiNi foams with reasonable mechanical properties. 1473 K (1200 °C) sintering experiments were carried out in two steps. Firstly specimens were heated to 1373 K (1100 °C) and held at that temperature for 0.5 hour. Then they were heated to 1473 K (1200 °C) and sintered for 2 hour. In order to see the effect of magnesium on oxidation and the corresponding secondary phase and liquid formation, a few specimen were produced by just consolidation of prealloyed TiNi powders and sintering them at 1373 K and 1473 K (1100 °C and 1200 °C) with and without using magnesium as getters.

Porosity content and density of TiNi foams were determined employing Archimedes' principle. Pore size and porosity distribution were determined using the commercial software Clemex Vision. Microstructural analysis was performed by a Jeol JSM 6400 scanning electron microscope (SEM) equipped with Noran System 6 energy dispersive X-ray spectroscopy (EDS). To study the thermal behavior of prealloyed TiNi powders, samples of 25 mg were heated up to 1473 K (1200 °C) at a rate of 10 °C/minutes under air and nitrogen (N_2) atmospheres in Setaram Setsys 1750 TG-DTA thermo gravimetric differential thermal analysis system. Phase transformation temperatures were determined employing a Perkin Elmer Diamond differential scanning calorimeter (DSC) with heating and cooling rates of 10 °C/minutes and under nitrogen atmosphere. Uniaxial compression tests were conducted using an Instron 3367, 30 kN capacity mechanical testing system, at ambient temperature ~298 K (~25 °C) and at a crosshead speed of 0.1 mm $minutes^{-1}$. Compression strains were measured using a clip on gage type extensometer while elastic moduli were calculated from least squares curves fitting to the linear portion of the stress–strain diagrams. Critical stresses corresponding to the initiation of stress induced martensitic transformations of the sintered samples were determined using the 0.2 pct-offset method.

III. RESULTS AND DISCUSSION

SEM images in Figures 1(a) to (d) show microstructure of TiNi alloy sintered at 1373 K (1100 °C) for 2 hour under protective argon atmosphere using high purity (99.99 pct) argon gas with titanium sponge as oxygen getter but without addition of any magnesium. Porous titanium/nickel oxide layers covering the surface of the powders are easily distinguishable. Apart from this oxide layer denoted as "a" in Figures 1(a) and (b), two other phases, labeled as "b" and "c" were detected. The compositions of these phases determined semi-quantitatively by energy-dispersive X-ray spectrometer (EDX) attached to SEM are listed in Table I and accordingly the phases present from the surface of the powder to the interior regions, *i.e.*, regions labeled as (a), (b) and (c), were determined to be, Ti_4Ni_2O, $TiNi_3$, and TiNi, respectively. Actually, in the absence of the oxygen contents due to the limitations of EDX, composition of the phase marked as "a" in Table I corresponds to Ti_2Ni as well as Ti_4Ni_2O and these phases cannot be distinguished even by X-ray or electron diffraction studies since both have an ordered

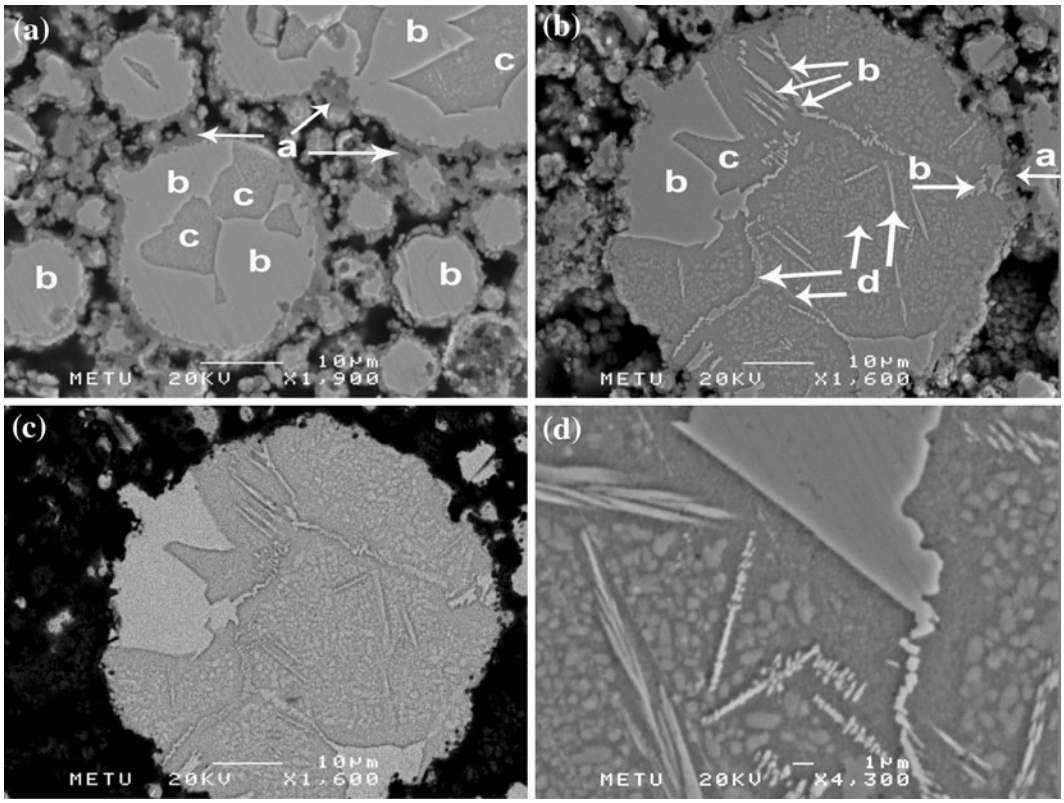

Fig. 1—SEM micrographs showing microstructural development in porous TiNi sintered at 1373 K (1100 °C) for 2 hour without using magnesium getters: (*a*) general view, (*b*) secondary electron, (*c*) backscattered electron images of an individual powder, and (*d*) morphologies of the phases present in TiNi at a higher magnification.

Table I. Chemical Compositions (at. pct) and Phase Identifications at Different Locations Shown in Fig. 1

	(a)	(b)	(c)
Ti	65.6 ± 3	27.9 ± 4	48.8 ± 1
Ni	34.4 ± 3	72.1 ± 4	51.2 ± 1
Phase identified	Ti_4Ni_2O	$TiNi_3$	TiNi

fcc structure of the Fe_3W_3C type and similar lattice parameters, namely, $a_0 = 1.13193$ nm for the former and $a_0 = 1.13279$ nm for the later.[30] In the current case, it is identified as Ti_4Ni_2O rather than Ti_2Ni because of the presence of $TiNi_3$ next to it. Ti_4Ni_2O is commonly observed in TiNi alloys in oxygenous atmosphere since solid solubility of oxygen in TiNi alloys is extremely small, around 0.045 at. pct,[31] and TiNi alloys with oxygen content exceeding this limit inevitably contains Ti_4Ni_2O phase. It is clear from Figure 1(a) that prealloyed TiNi powders, completely austenitic prior to sintering, are partly transformed during sintering because of the presence of oxygen. Powders with a diameter less than 10 μm have been found to consist of Ti_4Ni_2O and $TiNi_3$ phases only after the sintering operation and TiNi phase was observed to vanish totally. Indeed, Ti_4Ni_2O is not a distinct stoichiometric phase that appears on the TiNi-O phase diagram[32] at the sintering temperatures, but it is the Ti_2Ni phase with dissolved oxygen in it. Therefore, it may be more suitable to designate this solid-solution phase as $Ti_2Ni(O)_x$ ($0 \le x \le 0.5$). As during its formation in presence of oxygen, Ti atoms are consumed twice as much compared with Ni atoms in the matrix, $TiNi_3$ phase appears accompanying the $Ti_2Ni(O)_x$ phase in the Ni-enriched matrix. Overall transformation may be given as

$$TiNi + O_2 \rightarrow Ti_2Ni(O)_x + TiNi_3 \qquad [1]$$

Figure 1(b) shows that TiNi phase, marked as "c" both in Figures 1(a) and (b), actually embraces several phases with different morphologies in it and along its grain boundaries. EDX point analysis obtained from the dispersed phases marked as "d" were inconsistent because of deeper information depth and insufficient resolution (a few μm) of EDX analysis. They were identified as $TiNi_3$ despite lack of composition because the samples were cooled at the cold zone of the furnace at a rate of ~70 °C/minutes after sintering, which is similar to air cooling, and the precipitation of metastable Ti_3Ni_4 phase is not expected under such cooling conditions as confirmed by XRD studies (Figure 2). XRD results showed that beside Ti_4Ni_2O or $Ti_2Ni(O)_x$ phases TiO has also formed on the surface of the powders by the solid-state transformation given below:

$$Ti_2Ni(O)_x + O_2 \rightarrow TiO + [Ni] \qquad [2]$$

where [Ni] is that enriches Ti_2NiO_x which has a Ni solubility in the range of around 34 to 28 pct Ni at 1173 K (900 °C).[32]

It is noted from Figure 1 that during oxidation, not only oxygen atoms diffuse into powders but also excess nickel atoms, formed as a result of $Ti_2Ni(O)_x$ formation, diffuse from the surface to the interior regions, as has been proven with marker experiments,[33] using easy paths by dislocation and grain boundary diffusion mechanisms. There might be a difficulty in nucleation and subsequent growth of $TiNi_3$ as confirmed by its faceted interface formed with TiNi matrix. Thus, it prefers to nucleate heterogeneously on favorable sites present in the matrix.

In summary, oxidation process takes place in the current study in two steps:

In the first step, oxidation of TiNi (1) results in formation of $Ti_2Ni(O)_x$ and $TiNi_3$. Further oxidation of $Ti_2Ni(O)_x$ leads to formation of TiO and Ni. Ni phase has not been observed neither in XRD nor SEM studies meaning that it diffuses into interior parts and forms $TiNi_3$.

$Ti_2Ni(O)_x$ phase formation occurs at the initial stage of reaction between TiNi and oxygen in the shortest possible time.[32] Therefore, in the case of oxidation in air atmosphere, this stage would be of very short duration and difficult to observe. On the other hand, when the partial pressure of oxygen is reduced using vacuum or getters (Ti), metastable $Ti_2Ni(O)_x$ phase, which does not present in pseudo binary equilibrium TiNi-O phase diagram,[34] can be observed.

Selective oxidation of $Ti_2Ni(O)_x$ to lower oxides (TiO, Ti_2O_3, Ti_4O_7, *etc.*) can take place by the solid-state transformations.[32] Subsequently, the lower oxides are oxidized to higher ones resulting in a scale formation consisting of TiO_2, $NiTiO_3$, and Ni.[32] Further oxidation makes Ni to be oxidized and leads to the formation of NiO.[32,34] The type of oxide that is formed depends on the oxygen potential, *i.e.*, available oxygen amount and its partial pressure present in the system, or in other words, severeness of the oxidation as well as kinetic parameters. For example, complete oxidation of TiNi powder in air atmosphere at high temperatures for a sufficient time would lead to the formation of $NiTiO_3$, Ni(Ti), and TiO_2 phases.[32,34] However, oxidation at lower temperatures or oxidation of short duration would form TiO_2 or Ti_2O_3 or TiO phase besides $Ti_2Ni(O)_x$, $TiNi_3$, and TiNi. Relative amounts of all these phases may change; even some of them may completely disappear, depending on the oxidation kinetics and thermodynamic constraints.

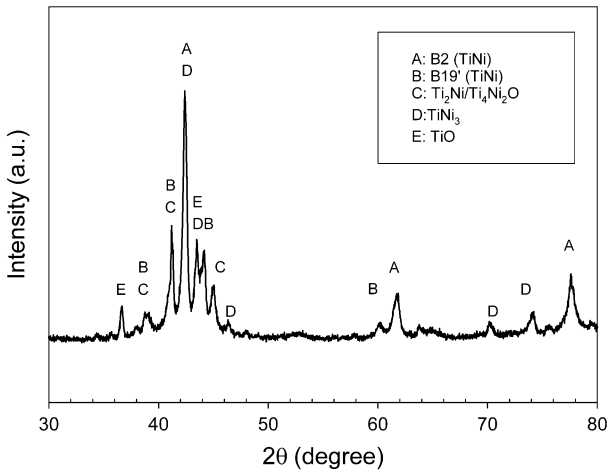

Fig. 2—XRD pattern of porous TiNi sintered at 1373 K (1100 °C) under argon gas atmosphere and using titanium getters.

Figure 3 presents microstructures developed in TiNi alloys sintered at 1373 K and 1473 K (1100 °C and 1200 °C) under protective magnesium vapor atmosphere. Sintering processes both lasting for 2 hour resulted in single B2 TiNi phase without any of the secondary intermetallics being present in Ti-Ni binary phase diagram or the contamination products such as oxides, nitrides, or carbonitrides. As is well known, oxidation of TiNi is a selective oxidation of Ti due to the large difference in the formation energies of the two oxides, namely: 691.5 and 674 kJ mol^{-1} for TiO_2, and 115.2 and 106.8 kJ mol^{-1} for NiO at 1373 K and 1473 K (1100 °C and 1200 °C), respectively. Partial pressure of oxygen must be less than 5×10^{-25} atm at 1373 K (1100 °C) and 10^{-23} atm at 1473 K (1200 °C) to prevent TiO_2 formation at the surface of the TiNi samples according to the calculations based on the thermodynamic data given in[35] for the oxidation reaction:

$$TiNi + O_2 \rightarrow TiO_2 + Ni \qquad [3]$$

High-purity argon or vacuum which is usually employed as the TiNi sintering atmosphere can decrease the oxygen partial pressure only down to 10^{-6} to

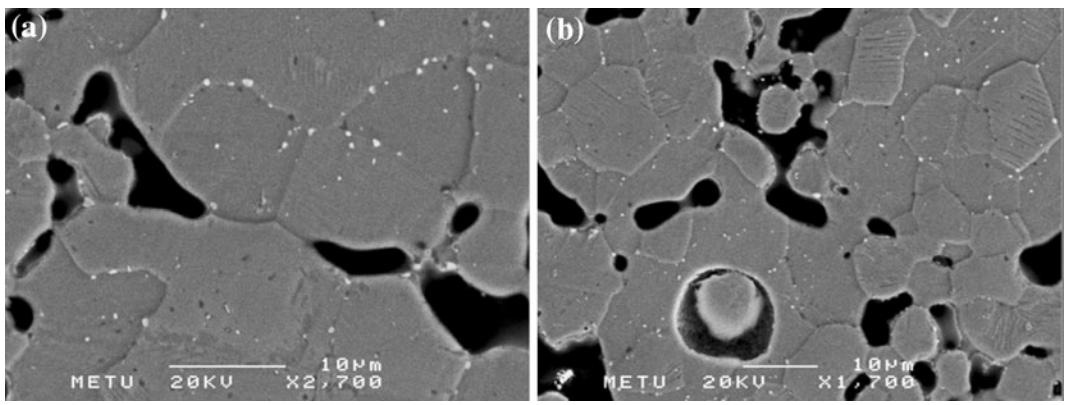

Fig. 3—SEM micrographs of specimens sintered at (*a*) 1373 K (1100 °C) and (*b*) 1473 K (1200 °C) for 2 h under magnesium vapor atmosphere.

10^{-8} atm which is still very high, and results in severe oxidation. Pure Ti used as getter can theoretically create extremely low oxygen partial pressures of 10^{-27} and 10^{-24} atm at 1373 K and 1473 K (1100 °C and 1200 °C), respectively, and thus can prevent the sample from oxidizing. However, in practice, such oxygen partial pressure levels may be difficult to accomplish because of leakages or atmosphere gases used. On the other hand, at 1373 K and 1473 K (1100 °C and 1200 °C), critical oxygen partial pressures for formation of MgO are 10^{-34} and 10^{-32} atm,[35] respectively, and these levels of oxygen partial pressure can reduce oxides of titanium effectively and thus prevent secondary phase formation.

Magnesium vapor does not only prevent secondary phase formation and contamination but also provides higher-temperature sintering opportunity. Foaming experiments with magnesium addition carried out at 1373 K (1100 °C) were successful; however, when the sintering temperature was increased to 1473 K (1200 °C), all the samples collapsed, Figure 4. An endothermic peak corresponding to 1393 K to 1398 K (1120 °C to 1125 °C) has been observed while conducting TG-DTA studies on the raw powders under air and nitrogen as atmosphere gases, Figure 5. Experiments under air atmosphere resulted in a white thick layer of oxide (probably TiO_2), while those under N_2 atmosphere caused formation of titanium nitride (TiN) in gold color. As seen from TG curves in Figure 6, mass gain was quite high for both the atmospheres used. Inductively coupled plasma-mass spectrometer (ICP-MS) and X-ray mapping were employed to ascertain the reason for the appearance of the peak at 1393 K to 1398 K (1120 °C to 1125 °C). Since the ICP-MS results confirmed the compositions of TiNi powders as stated by the suppliers, and X-ray mapping did not point out a compositional inhomogeneity, it was concluded that oxidation occurring during heating and cooling cycles of DTA was responsible for the partial melting. Zhang and his co-workers[27] also detected an endothermic peak at 1397 K (1124 °C) in DTA experiments carried out under the Ar-1 pct H_2 gas mixture which provides an oxygen partial pressure in the range 10^{-12} to 10^{-15} atm at the temperature range of 1373 K to 1473 K (1100 °C to 1200 °C). The peak totally disappeared when they used titanium getters to clean the gas mixture and provided a better protective atmosphere.

Selective oxidation of titanium results in nickel release in TiNi matrix, and the nickel content increases according to the solid-state phase transformations (1 to 3) in the regions close to the surface of the powders. When the nickel content reaches to eutectic regime (57 pct Ni at. to 75 pct Ni at.), appearance of liquid phase is inevitable at 1391 K (1118 °C) and higher temperatures. Therefore, it is essential to prevent oxidation of TiNi powders for high-temperature [>1391 K (1118 °C)] sintering practices. As depicted before, at 1373 K and 1473 K (1100 °C and 1200 °C), Mg gives a critical oxygen partial pressure of around 10^{-34} and 10^{-32} atm, respectively, and it does not only reduce the oxides of titanium but also prevents liquid phase formation and enables employment of higher sintering temperatures. Magnesium is much more effective in these issues than

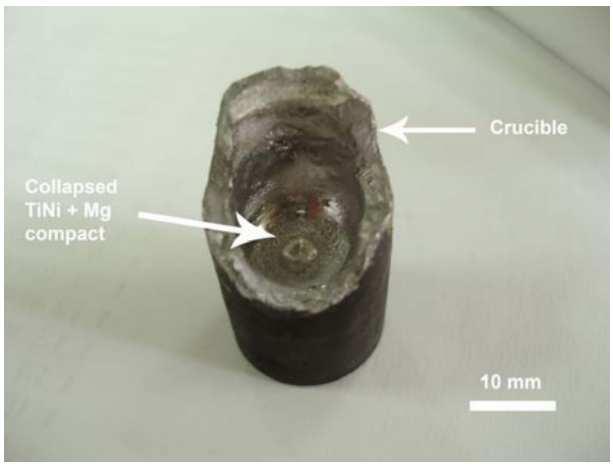

Fig. 4—TiNi + Mg compact collapsed onto the base of the crucible as a result of direct heating to the sintering temperature of 1473 K (1200 °C).

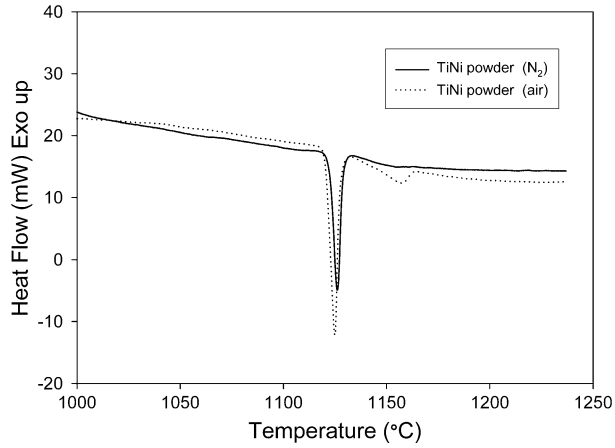

Fig. 5—DTA curves of prealloyed powders used, under air and nitrogen atmospheres.

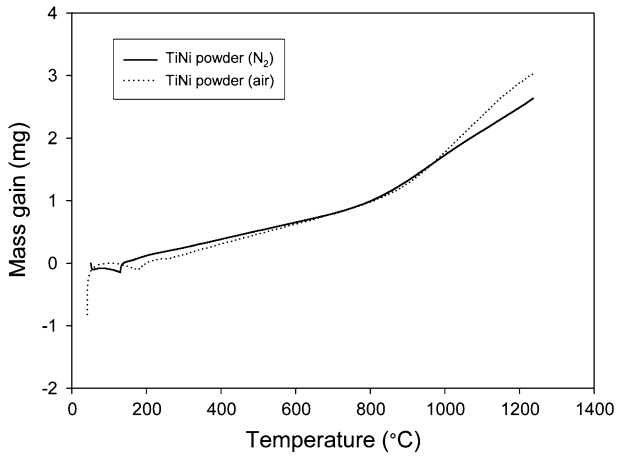

Fig. 6—TG curves of prealloyed TiNi powders under air and nitrogen atmospheres.

titanium getters. For example, Ar-1 pct H_2 gas mixture + titanium getters used in Zhang and his colleagues' study[27] effectively avoided the liquid phase formation but could not prevent secondary phase formation. The thickness of the layer affected as a result of oxidation was 100 μm, and Ti_4Ni_2O, $TiNi_3$ as well as TiO_2 were the phases formed. Moreover, from the end of the oxidation layer to the interior regions, $TiNi_3$ precipitates in TiNi matrix were observed, implying that the actual oxidation layer affected was greater than 100 μm in fact. On the other hand, sintered TiNi foams prepared from prealloyed powders, with 21 μm size on average, under magnesium vapor atmosphere in the current study did not show any secondary intermetallics or oxide compounds.

As TiNi starts to oxidize rapidly at 473 K (200 °C),[34] direct heating of compacted samples to 1473 K (1200 °C) resulted in their collapse because of the liquid phase formation at the eutectic temperature of 1391 K (1118 °C). Pure magnesium starts to melt at 923 K (650 °C), and its vapor pressure increases with increasing temperature. TiNi alloy oxidizes up to this temperature starting from 473 K (200 °C), because solid magnesium is not sufficiently effective in preventing oxidation. Liquid or vapor magnesium [1363 K (1090 °C)], on the other hand, reacts severely with oxygen spreading onto TiNi powder surfaces through sintering process. Magnesium could not reduce the oxides of TiNi powders and prevent the powder surface from nickel enrichment because of enough time not being available during the course of rapid heating. However, holding the sample at 1373 K (1100 °C) for 30 minutes was sufficient to prevent the shift to eutectic composition. Subsequently, sintering done at 1473 K (1200 °C) resulted in sound, Figure 7(a), chemically homogeneous TiNi foams free from secondary intermetallics and contamination products, Figure 7(b). By means of this two-step processing, magnesium may allow sintering probably up to the melting point of TiNi. Other TiNi foam production techniques, especially HIP, despite allowing elevated temperature sintering [>1391 K (1118 °C)] using titanium getters, fail in preventing secondary phase formation and contamination, which results in brittleness of the foams.

TiNi foams with different porosities all exhibited single distinct peak (not given here) during both heating and cooling,[22] and transformation temperatures were found to be higher than those of the raw powder. Martensite start temperatures measured by DSC of the foams were lower than room temperature, thus insuring that the samples used in compression tests were in completely austenitic state.[22]

Figure 8 presents the compressive stress–strain curves of the as-processed TiNi foams with various porosity contents and sintered at different temperatures. In the current study, the horizontal plateau region that normally occurs in highly porous metallic foams[36] and bulk TiNi alloys[31] has not been observed, especially for the samples sintered at 1373 K (1100 °C) as shown in Figure 8(a). This can be attributed to the pore-type and the distribution of neck size. Open cells foams (high porosity samples) have a well-defined plateau stress because the cell edges and walls yield in bending, resulting in plastic collapse or buckling of the foam. Plastic collapse occurs when the moment exerted on the cell walls exceeds the fully plastic moment creating plastic hinges. However, closed cell foams show more complicated behavior which can cause the stress to rise with increasing strain because the cell faces are subjected to tensile stresses during compression.[36] Low porosity or high relative density foams have closed pores or cells. As a result, the plateau regions of the stress–strain curves are not flat and a slope increasing with decreasing porosity occurs. Every sintering neck formed randomly as a result of geometrical relations among the raw prealloyed powders actually behaves as a small compression sample of different shape, dimension and orientation experiencing the different stress even though the applied gross load is the same. Phase transformations occurring during loading therefore cannot take place at constant stress levels. However, higher sintering temperature [1473 K (1200 °C)] resulted in the

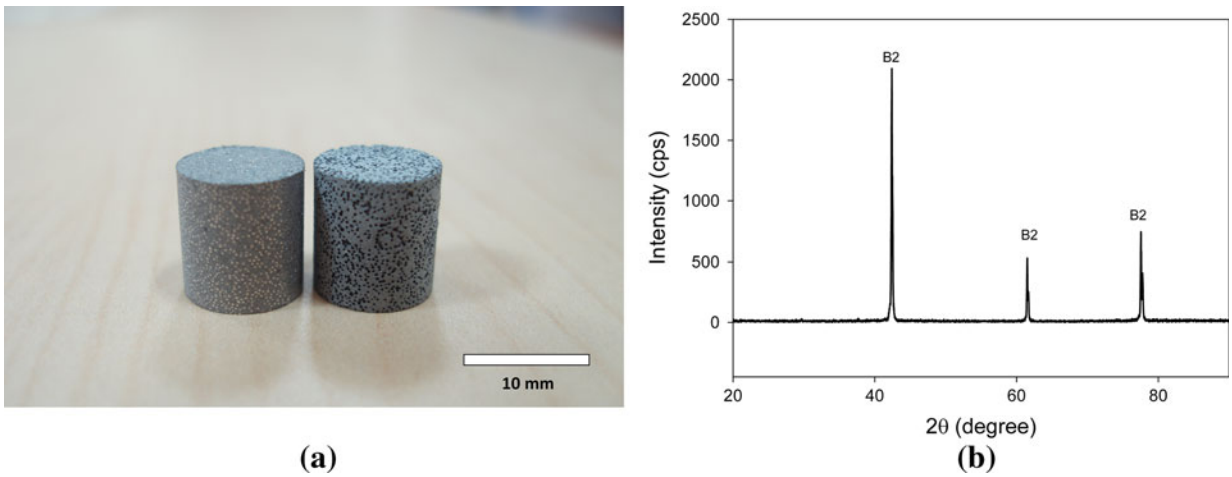

Fig. 7—(*a*) Macrograph, showing white coarse Mg powders distributed randomly among dark fine TiNi powders after compaction step at left side and the processed foam at right side, and (*b*) XRD pattern of 62 pct porous Ti-50.6 at. pct Ni foam sintered at 1473 K (1200 °C) for 2 h.

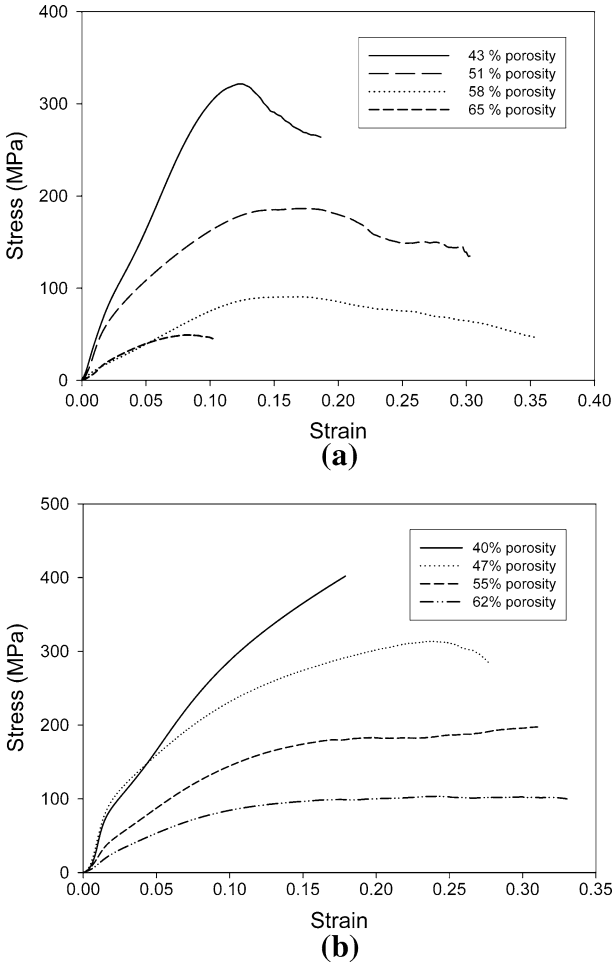

Fig. 8—Stress–strain curves of TiNi foams produced by sintering at (*a*) 1373 K (1100 °C) and (*b*) 1473 K (1200 °C) for 2 h.

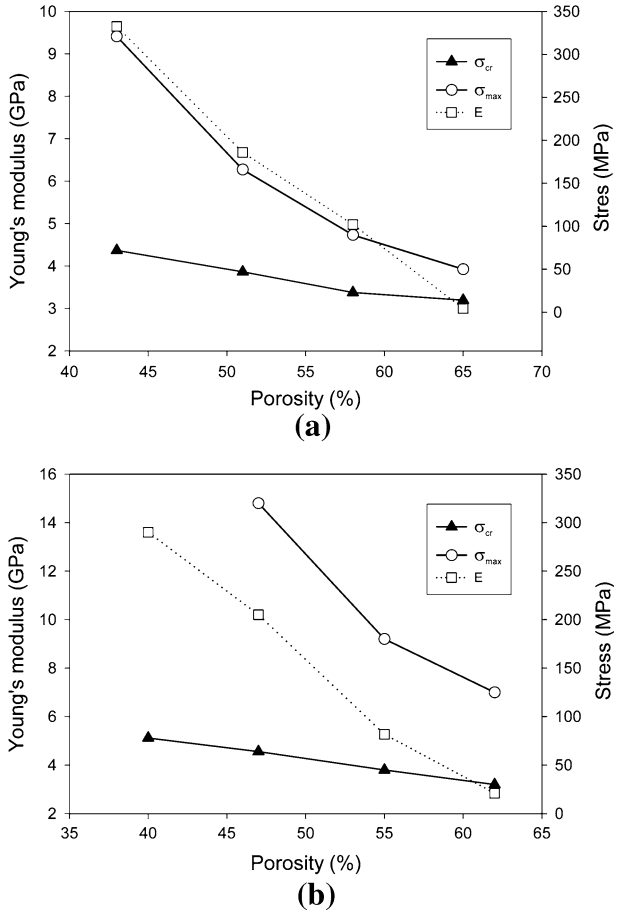

Fig. 9—Effect of porosity on elastic moduli (E), compression strength (σ_{max}), and critical stress for inducing martensite (σ_{cr}) in TiNi foams sintered at (*a*) 1373 K (1100 °C) and (*b*) 1473 K (1200 °C) for 2 h.

appearance of horizontal plateau stage because of stronger sintering necks at relatively lower porosity levels such as 47, 55, and 62 pct as seen from Figure 8(b). It should be noted that 40 pct porous sample in the figure could not be subjected to a full compression test because of the limitations of the capacity of the equipment used.

Mechanical properties of the foams produced by sintering at 1373 K (1100 °C) for 2 hour, as obtained from compression tests, are summarized in Figure 9(a), where E represents Young's modulus, whereas σ_{cr} designates the critical stress for inducing martensite (yield strength for bone) and σ_{max} is the compressive strength. TiNi alloy foams with 58 pct porosity appear to be appropriate for cancellous bone replacement applications, while TiNi foams with relatively lower porosities, 51 pct and less, were found to be appropriate for both cancellous ($E = 1 \pm 0.8$ GPa, $\sigma_{cr} = 15 \pm 8$ MPa, and $\sigma_{max} = 25 \pm 8$ MPa[37]) and cortical bone ($E = 12$ to 17 GPa, $\sigma_{cr} = 105$ to 121 MPa, and $\sigma_{max} = 156$ to 212 MPa[36,37]) replacement applications, Figure 9(a). TiNi foams sintered at 1473 K (1200 °C) and with porosities in the range of 40 to 55 pct are also acceptable to be used as implant materials, whereas 62 pct porous TiNi is insufficient in strength (125 MPa), Figure 9(b). However, sintering at higher temperatures, for example 1523 K (1250 °C), may improve the strength by eliminating the micropores present in the cell walls. For example, 1473 K (1200 °C) sintering operation compared with sintering done at 1373 K (1100 °C) reduced the microporosity content by around 3 to 4 pct as presented in Table II. It should be well understood that the mechanical properties of TiNi foams produced by different processing routes cannot be compared directly just considering their porosity ratio, because pore characteristics (*i.e.*, pore-type, pore morphology, pore size, distribution, *etc.*); microstructure (*i.e.*, morphology and size of phases present, grain size, *etc.*); oxidation and other contamination levels; post-processing operations such as aging and solutionizing heat treatments; and deformation. Phase transformation temperatures and test temperatures also greatly change the deformation behavior and mechanical properties. This can be clearly observed from results of the current study in which the only variable is sintering neck characteristics. The sintering at 1473 K (1200 °C) increased the strength and elastic moduli values dramatically for the samples produced by adding same amount of magnesium. For example, σ_{max} for 65 pct porous sample is lower than 60 MPa, while it is 125 MPa for 62 pct porous sample. In addition, 47

Table II. Effects of Mg Addition and Sintering Temperature on Total, Macro, and Microporosities

Percentage of Mg Added	Percentage of Total Porosity by Density Measurements	Percentage of Microporosity Calculated	Sintering Temperature K (°C)
30	43	13	1373 (1100)
40	51	11	
50	58	8	
60	65	5	
30	40	10	1473 (1200)
40	47	7	
50	55	5	
60	62	2	

and 43 pct porous samples have similar σ_{max} values around 300 MPa, although the former has higher porosity. This is also valid for 55 and 51 pct porous specimens as seen readily from Figures 9(a) and (b). Sintering at 1473 K (1200 °C) also improved the ductility for strain levels from the range of 8 to 14 pct up to that of 20 to 23 pct, Figure 8. Ductility has been accepted as the strain corresponding to stress level at which first crack occurs in this study, because ductile porous metallic alloys do not fracture suddenly even at very high strains in compression. As sintering at 1473 K (1200 °C) results in stronger and more homogeneous sintering necks, the foams produced under this condition exhibited greater ductility. As compression tests presented in the literature are generally not carried out up to fracture, it is impossible to compare ductility results, as well as compression strength.

IV. CONCLUSIONS

Magnesium powders have been used as both reductant and space holder material in the processing of TiNi foams via conventional powder metallurgy route starting from prealloyed TiNi powders. Main conclusions that can be drawn from this study are as follows:

1. Ti getters + Ar gas atmosphere is not adequate to prevent secondary phase formation during sintering of TiNi prealloyed powders.
2. Main solid-state phase transformations involved in oxidation of TiNi powders under Ti getters + Ar gas atmosphere are $TiNi + O_2 \rightarrow Ti_2Ni(O)_x + TiNi_3$ and $Ti_2Ni(O)_x + O_2 \rightarrow TiO + [Ni]$.
3. Magnesium can prevent effectively formation of secondary intermetallic phases as it is capable of providing extremely lower partial pressure of oxygen level, 10^{-34} atm, at a classical sintering temperature of 1373 K (1100 °C).
4. Magnesium vapor introduced into the sintering atmosphere does not only prevent secondary phase formation and contamination but also provide higher-temperature sintering opportunity. By means of two-step sintering processing [holding the sample at 1373 K (1100 °C) for 30 minutes and subsequently sintering at temperatures higher than the eutectic temperature, 1391 K (1118 °C)], magnesium may allow sintering to proceed probably up to the melting point of TiNi.
5. Two-step sintering procedure improves the strength, ductility, and Young's modulus of TiNi foams by minimizing microporosity and forming stronger sintering necks and more homogeneous macropores or cell walls.

ACKNOWLEDGMENT

The authors gratefully acknowledge the partial funding support provided to this research by The Scientific and Technological Research Council of Turkey (TUBITAK) under Grant No: 108M118.

REFERENCES

1. A. Bansiddhi, T.D. Sargeant, S.I. Stupp, and D.C. Dunand: *Acta Biomater.*, 2008, vol. 4, pp. 773–82.
2. V.E. Gjunter, P. Sysoliatin, and T. Temerkhamor: *Superelastic Shape Memory Implants in Maxillofacial Surgery, Traumatology, Orthopaedics, and Neurosurgery*, 1st ed., Tomsk University Publishing House, Tomsk, 1995, p. 14.
3. V. Itin, V. Gyunter, S. Shabalovskaya, and R. Sachdeva: *Mater. Charact.*, 1994, vol. 32, pp. 179–87.
4. S.L. Zhu, X.J. Yang, D.H. Fu, L.Y. Zhang, C.Y Li, and Z.D. Cui: *Mater. Sci. Eng. A*, 2005, vol. 408, pp. 264–68.
5. S.K. Sadrnezhaad, H. Arami, H. Keivan, and R. Khalifezadeh: *Mater. Manuf. Processes*, 2006, vol. 21, pp. 727–35.
6. B. Bertheville: *Biomaterials*, 2006, vol. 27, pp. 1246–50.
7. T. Aydoğmuş and A.Ş. Bor: *Turkish J. Eng. Env. Sci.*, 2011, vol. 35, pp. 69–82.
8. B. Yuan, X.P. Zhang, C.Y. Chung, M.Q. Zeng, and M. Zhu: *Metall. Mater. Trans. A*, 2006, vol. 37A, pp. 755–61.
9. B.Y. Li, L.J. Rong, Y.Y. Li, and V.E. Gjunter: *Acta Mater.*, 2000, vol. 48, pp. 3895–04.
10. D.C. Lagoudas and E.L. Vandygriff: *J. Intell. Mater. Syst. Struct.*, 2002, vol. 13, pp. 837–50.
11. S. Wu, C.Y. Chung, X. Liu, P.K. Chu, J.P.Y. Ho, C.L. Chu, Y.L. Chan, K.W.K. Yeung, W.W. Lu, K.M.C. Cheung, and K.D.K. Luk: *Acta Mater.*, 2007, vol. 55, pp. 3437–51.
12. B. Yuan, C.Y. Chung, P. Huang, and M. Zhu: *Mater. Sci. Eng., A*, 2006, vols. 438–440, pp. 657–60.
13. X.P. Zhang, H.Y. Liu, B. Yuan, and Y.P. Zhang: *Mater. Sci. Eng., A*, 2008, vols. 481–482, pp. 170–73.
14. Y. Zhao, M. Taya, Y. Kang, and A. Kawasaki: *Acta Mater.*, 2005, vol. 53, pp. 337–43.
15. D.S. Grummon, J.A. Shaw, and A. Gremillet: *Appl. Phys. Lett.*, 2003, vol. 82, pp. 2727–29.
16. H. Guoxin, Z. Lixiang, F. Yunliang, and L. Yanhong: *J. Mater. Process. Technol.*, 2008, vol. 206, pp. 395–99.
17. Y.P. Zhang, B. Yuan, M.Q. Zeng, C.Y. Chung, and X.P. Zhang: *J. Mater. Process. Technol.*, 2007, vols. 192–193, pp. 439–42.
18. Y.P. Zhang, D.S. Li, and X.P. Zhang: *Scr Mater*, 2007, vol. 57, pp. 1020–23.

19. D.S. Li, Y.P. Zhang, G. Eggeler, and X.P. Zhang: *J. Alloys Compd.*, 2009, vol. 470, pp. L1–L5.
20. A. Bansiddhi and D.C. Dunand: *Intermetallics*, 2007, vol. 15, pp. 1612–22.
21. A. Bansiddhi and D.C. Dunand: *Acta Biomater.*, 2008, vol. 4, pp. 1996–07.
22. T. Aydoğmuş, E.T. Bor, and Ş. Bor: *Metall. Mater. Trans. A*, 2011, vol. 42A, pp. 2547–55.
23. L. Krone, E. Schuller, M. Bram, O. Hamed, H.P. Buchkremer, and D. Stover: *Mater. Sci. Eng., A*, 2004, vol. 378, pp. 185–90.
24. J. Mentz, M. Bram, H.P. Buchkremer, and D. Stover: *Adv. Eng. Mater.*, 2006, vol. 8, pp. 247–52.
25. E. Schuller, L. Krone, M. Bram, H.P. Buchkremer, and D. Stover: *J. Mater. Sci.*, 2005, vol. 40, pp. 4231–38.
26. T. Aydoğmuş and Ş. Bor: *J. Alloys Compd.*, 2009, vol. 478, pp. 705–10.
27. J. Zhang, G. Fan, Y. Zhou, X. Ding, K. Otsuka, K. Nakamura, J. Sun, and X. Ren: *Acta Mater.*, 2007, vol. 55, pp. 2897–05.
28. B. Bertheville: *Mater. Trans.*, 2006, vol. 47, pp. 698–03.
29. B. Bertheville and J.E. Bidaux: *J. Alloys Compd.*, 2005, vol. 387, pp. 211–16.
30. M. Nishida, C.M. Wayman, and T. Honma: *Metall. Mater. Trans. A*, 1986, vol. 17A, pp. 1505–15.
31. K. Otsuka and C.M. Wayman: *Shape Memory Materials*, 1st ed., Cambridge University Press, Cambridge, 1998, pp. 49–96.
32. V.G. Chuprina and I.M. Shalya: *Powd. Metall. Met. Cer.*, 2002, vol. 41, pp. 85–89.
33. S. Schirmer, J.K.N. Lindner, and S. Mandl: *Nucl. Instrum. Methods Phys. Res. B*, 2007, vol. 257, pp. 714–17.
34. G.S. Firstov, R.G. Vitchev, H. Kumar, B. Blanpain, and J. Van Humbeeck: *Biomaterials*, 2002, vol. 23, pp. 4863–71.
35. I. Barin: *Thermochemical Data of Pure Substances*, 1st ed., VCH Verlagsgeselischaft, Weinheim, 1989, pp. 1083–46.
36. L.J. Gibson and M.F. Ashby: *Cellular Solids: Structure and Properties,* 2 nd ed, Cambridge University Press, Cambridge, 1997, pp. 429–52.
37. M. Elices: *Structural Biological Materials. Design and Structure-property Relationships*, Pergamon press, Oxford, 2000, pp. 31–72.